CD44-hyaluronan axis plays a role in the interactions between colon cancer-derived extracellular vesicles and human monocytes

ANETA BABULA[1,2], ADRIANNA GAŁUSZKA-BULAGA[1], KAZIMIERZ WĘGLARCZYK[1], MACIEJ SIEDLAR[1] and MONIKA BAJ-KRZYWORZEKA[1]

[1]Department of Clinical Immunology, Institute of Pediatrics, Jagiellonian University Medical College, 30-663 Kraków; [2]Doctoral School of Medical and Health Sciences, Jagiellonian University Medical College, 31-530 Kraków, Poland

Received February 19, 2023; Accepted July 17, 2023

DOI: 10.3892/ol.2023.13999

Abstract. During tumor progression, monocytes circulating in the blood or infiltrating tissue may be exposed to tumor-derived extracellular vesicles (TEVs). The first stage of such interactions involves binding of TEVs to the surface of monocytes, followed by their internalization. The present study examines the role of CD44 molecules in the interactions between monocytes and EVs derived from colon cancer cell lines (HCT116 and SW1116). The efficiency of the attachment and engulfment of TEVs by monocytes is linked to the number of TEVs and time of exposure/interaction. The two investigated TEVs, $TEVs_{HCT116}$ and $TEVs_{SW1116}$, originating from HCT116 and SW1116 cells, respectively, differ in hyaluronan (HA) cargo, which reflects HA secretion by parental cancer cells. HA-rich $TEVs_{HCT116}$ are internalized more effectively in comparison with HA-low $TEVs_{SW1116}$. Blocking of CD44 molecules on monocytes by anti-CD44 monoclonal antibody significantly decreased the engulfment of $TEVs_{HCT116}$ but not that of $TEVs_{SW1116}$ after 30 min contact, suggesting the involvement of the HA-CD44 axis. The three subsets of monocytes, classical, intermediate and non-classical, characterized by gradual changes in the expression of CD14 and CD16 markers, also differ in the expression of CD44. The highest expression of CD44 molecules was observed in the intermediate monocyte subset. Blocking of CD44 molecules decreased the internalization of HA-rich TEVs in all three subsets, which is associated with CD44 expression level. It was hypothesized that HA carried by TEVs, potentially as a component of the 'corona' coating, may facilitate the interaction between subsets of monocytes and TEVs, which may influence the fate of TEVs (such as the rate of TEVs adhesion and engulfment) and change monocyte activity.

Correspondence to: Dr Monika Baj-Krzyworzeka, Department of Clinical Immunology, Institute of Pediatrics, Jagiellonian University Medical College, 265 Wielicka, 30-663 Kraków, Poland
E-mail: monika.baj-krzyworzeka@uj.edu.pl

Key words: monocyte, CD44, hyaluronan, extracellular vesicles, colon cancer

Introduction

Extracellular vesicles (EVs) are a heterogeneous population of membrane vesicles released by almost all types of cells. Increased secretion of EVs is observed in cases of intensively proliferating tumor cells. EVs carry biologically important components including proteins, nucleic acids, lipids and glycans (1) located within EVs or as corona biomolecules surrounding EVs (2). Colon cancer-derived EVs express parental cancer-associated markers such as epithelial cell adhesion molecule, glypican 1 and mucin 13 (3-5). After secretion from cancer cells, tumor-derived EVs (TEVs) can be taken up by neighboring cells or circulate freely within body fluids (6). Interest in TEVs has developed due to their impact on phenotype and function of acceptor/target cells.

Effective transfer of TEVs to monocytes has been described (7-9), however, the knowledge of the early stages of these interactions is limited. In general, membrane fusion and different types of endocytosis, which may occur simultaneously but with different effectiveness, are essential for uptake of TEVs (10). Monocytes and macrophages preferentially use phagocytosis, a type of endocytosis dedicated to the internalization of particles in a receptor-dependent manner (11). The major phagocytic receptors are Fc receptors (CD64, CD32 and CD16), complement and scavenger receptors widely distributed on immune cells (12). In 2006, Vachon *et al* (13) showed that CD44 is a competent receptor that efficiently mediates internalization of hyaluronan (HA)-coated beads. CD44 is the major receptor for HA, a negatively-charged polysaccharide composed of glucuronic acid and N-acetylglucosamine units. It is hypothesized that the CD44 molecule may be involved in the engulfment of small-size TEVs (<200 nm) and that HA carried by TEVs may facilitate TEVs interactions with CD44-expressing cells. All monocytes express CD44 molecules, with the predominance of short, standard form CD44s encoded by exons 1-5 and 16-20 (14). Monocytes are a heterogeneous population of cells differing in phenotype and functions (15,16). In 2010, Ziegler-Heitbrock *et al* (15) proposed a nomenclature for monocyte subpopulations based on expression of markers CD14 and CD16. The major monocyte subset characterized by high expression of CD14 marker is classical monocytes. The minor monocyte subset with low CD14 and high CD16 is non-classical monocytes. Cells in

between these two subpopulations are intermediate monocytes (15). Different subsets of monocytes serve different roles during tumor progression; for example, following migration from the bloodstream, classical monocytes mainly differentiate into pro-tumoral tumor-associated macrophages (TAMs), non-classical monocytes prevent metastasis formation (17) and the intermediate subset supports angiogenesis (18). The knowledge concerning CD44 expression in the aforementioned monocyte subsets (19) is limited, however, it may be important when considering their interactions with tumor cells and TEVs.

It was previously shown that blocking monocytic CD44 molecules with anti-CD44 antibodies decreases the engulfment of large-size (>200 nm) TEVs of pancreatic carcinoma origin (20). The present study aimed to investigate the role of CD44 in the internalization of small TEVs of colon cancer origin. It is hypothesized that CD44 plays a role in TEVs endocytosis by monocytes, varies between subsets of monocytes and that the composition of TEVs impacts the rate of this process.

Material and methods

Cell culture and isolation of TEVs. TEVs were obtained from supernatant derived from the culture of the colon cancer cell lines SW1116 and HCT116 (American Type Culture Collection). Briefly, cells were cultured at 37˚C, without CO_2 (SW1116) or with 5% CO_2 (HCT116) in L15 or McCoy's medium (cat. nos. 11415064 and 16600082; Gibco; Thermo Fisher Scientific, Inc.), respectively, with 10% fetal bovine serum (FBS; cat. no. S1860; Ultra-low Endotoxin; Biowest USA). Cells were split twice per week. Bovine-derived EVs were depleted from FBS by centrifugation at 100,000 x g for 4 h at 4˚C (Sorvall™ WX+ Ultracentrifuge with T-1270 rotor; Thermo Fisher Scientific, Inc.). PBS used in TEVs isolation was filtered (0.22 μm; Merck KGaA) and its purity was tested by nanoparticle tracking analysis (NTA; NanoSight LM10HS equipped with the LM14 488 nm laser module; Malvern Instruments, Ltd.). Cell lines were tested every month for Mycoplasma sp. contamination using a Mycoplasma PCR Detection kit according to manufacturer's instructions (cat. no. G238; Applied Biological Materials, Inc.). Supernatants from well-grown (confluency >90%) cell cultures were collected and spun at 500 x g for 5 min at room temperature (RT), and then at 3,200 x g for 12 min at 4˚C to remove cell debris. The supernatants were again centrifuged at 100,000 x g for 2 h at 4˚C. Pellets were washed in PBS to remove FBS and resuspended in filtered PBS. Quantification of TEVs was performed by NTA and protein measurement by the Bradford method (cat. no. 5000201; Bio-Rad Laboratories, Inc.). TEVs were tested for endotoxin contamination by Limulus test according to the manufacturer's instructions (cat. no. A39553; Pierce™ Chromogenic Endotoxin Quant kit; Thermo Fisher Scientific, Inc.), and stored at -80˚C.

Isolation of monocytes. Anticoagulated citrate dextrose A-treated blood from healthy donors was purchased from the Regional Center of Blood Donation and Blood Therapy (Krakow, Poland; agreement no. DZM/SAN/CM/U-678/2015; Bioethical Committee of the Jagiellonian University, Kraków, Poland; approval no. 1072.6120.1.2020). Human peripheral blood mononuclear cells were isolated from blood by standard Ficoll/Isopaque (cat. no. 17-1440-03; GE Healthcare) density gradient centrifugation (30 min, 800 x g, RT). Monocytes were separated from mononuclear cells by counterflow centrifugal elutriation with a JE-5.0 elutriation system equipped with a 5-ml Sanderson separation chamber (Beckman Coulter, Inc.), as previously described (21). Monocytes were suspended in RPMI-1640 culture medium supplemented with L-glutamine (cat. no. 11875093; Gibco; Thermo Fisher Scientific, Inc.) and gentamicin (cat. no. P06-13021; 50 μl/ml; PAN-Biotech GmbH). The purity of isolation was ≥95%, determined by staining with an anti-CD14 monoclonal antibody (cat. no. 555399; mAb; clone no. M5E2; BD Pharmingen; BD Biosciences). Monocytes were incubated with anti-CD14 for 30 min at 4˚C in the dark (antibody concentration according to the manufacturer's protocol) and then washed with PBS, collected by flow cytometry (BD FACSCanto™; BD Biosciences) and analyzed by FACSDiva Software (version 8.0.1; BD Biosciences).

Expression of CD44 on monocytes and subpopulations. To determine the expression of surface markers on monocytes by flow cytometry, the following mAbs were used: FITC anti-human CD44s (cat. no. 347943; clone no. G44-26), APC anti-human CD14 (cat. no. 555399; clone no. M5E2) and PE anti-human CD16 (cat. no. 555407; clone no. 3G8) (BD Pharmingen; BD Biosciences). Monocytes were incubated with anti-CD44, -CD14 and -CD16 for 30 min at 4˚C in the dark and then washed with PBS as aforementioned. A total of 10,000 cells per run were analyzed on a BD FACSCanto™ Flow Cytometer (BD Biosciences) using Diva Software (version 8.0.1; BD Biosciences). The monocyte subsets gating strategy is presented in Fig. S1. CD44 is used throughout the manuscript in the sense of CD44s, unless otherwise noted. CD44 expression was analyzed as mean fluorescence intensity (MFI) because the percentage of cells that exhibited fluorescence in every subpopulation was ~100%. CD44 expression on monocytes was evaluated after 2 and 18 h of culture (control), as well as after incubation with TEVs (TEV:monocyte, 5,000:1) after the same times, at 37˚C.

TEVs characterization. The size and concentration of TEVs were defined by NTA. A suspension of 1,000 times diluted TEVs was loaded into the measuring chamber. The movement of particles was recorded in triplicates of 1-min videos (Fig. S2), after which the concentration, average size and mode values of TEVs were calculated. TEVs membrane structure was confirmed by MEMGlow staining, as previously described (22). MEMGlow solution (cat. no. MG01-02; 20 μM; Cytoskeleton, Inc.) was diluted in filtered PBS to 0.1 μM concentration, added to 40X diluted TEVs suspension and incubated for 30 min at RT in the dark. It was later analyzed by flow cytometry without washing.

EV markers were detected by western blotting (WB). Briefly, protein concentration in EV samples was determined by the Bradford method. Next, 20 μg/lane EV proteins extracted with Mammalian Protein Extraction Reagent (cat. no. 78501; Thermo Fisher Scientific, Inc.) were heated with loading buffer at 75˚C for 10 min (cat. no. NP0007; 4X sample buffer; and cat. no. NP0004; 10X sample

reducing agent; Invitrogen, Thermo Fisher Scientific, Inc.). Electrophoresis was performed at 180 V for 45 min on 14% polyacrylamide gel. Proteins were transferred onto a polyvinylidene fluoride membrane with semi-dry transfer at 25 V for 1 h, blocked at RT for 1 h with 1% bovine serum albumin in Tris-buffered saline with 0.1% Tween and incubated overnight at 4˚C with rabbit anti-CD9 (cat. no. 13174S; clone no. D801A), anti-β-actin (cat. no. 8457S; clone no. D6A8) and mouse anti-ALIX mAb (cat. no. 2171S; clone no. 3A9) (Cell Signaling Technology, Inc.) diluted 1,000 times. Next, the membrane was incubated with secondary anti-rabbit (cat. no. sc-2357; Santa Cruz Biotechnology, Inc.) or anti-mouse (cat. no. 31430; Invitrogen; Thermo Fisher Scientific Inc.) antibodies conjugated with horseradish peroxidase and diluted 2,000 times for 1 h at RT. The protein bands were visualized with SuperSignal™ West Pico PLUS Chemiluminescent Substrate (cat. no. 34578; Thermo Fisher Scientific, Inc.) by ChemiDoc Imaging System (Bio-Rad Laboratories, Inc.).

The expression of CD44 and CD44v6 on TEVs was determined by flow cytometry with mAbs: FITC anti-human CD44 and PE anti-human CD44v6 (cat. no. 566803; clone no. 2F10). TEVs were incubated with CD44 and CD44v6 for 30 min at 4˚C in the dark and analyzed on a BD FACSCanto™ Flow Cytometer (BD Biosciences).

TEVs staining. TEVs suspension was incubated with SYTO RNASelect (cat. no. S32703; Thermo Fisher Scientific, Inc.) at 37˚C for 20 min in the dark. Excess dye was removed with Exosome Spin Columns (cat. no. 4484449; Invitrogen, Thermo Fisher Scientific, Inc.) according to the manufacturer's protocol. The effectiveness of labeling was determined by flow cytometry (FACS Canto II; BD Biosciences) in the FL1 channel (Fig. S3). SYTO RNASelect-labeled TEVs were termed SYTO RNA-labeled TEVs.

HA content measurement. HA concentration in cell culture supernatants, TEVs and culture supernatants after TEVs isolation was measured by Quantikine ELISA Hyaluronan kit (cat. no. DHYAL0; R&D Systems, Inc.) according to the manufacturer's protocol. Briefly, samples were diluted 20-50-fold, depending on the HA content. The optical density was determined with ELX800NB, Universal Microplate Reader (450 nm; BioTek Instruments, Inc.). The concentration of HA was calculated by linear standard curve. The minimum detectable dose of HA was 0.068 ng/ml.

Transfer of TEVs to monocytes and monocyte subsets. SYTO RNA-labeled TEVs were incubated with monocytes at a ratio of 1,000:1; 5,000:1 and 10,000:1 for 30 min, 2 h and overnight at 37˚C. Following incubation, cells were washed and analyzed by flow cytometry. The binding of SYTO RNA-labeled TEVs to monocytes was determined by analysis of green fluorescence intensity and percentage of positive cells. Vital dye trypan blue was used for quenching extracellular fluorescence, as previously described (23). Briefly, 100 μl cell suspension was mixed with trypan blue solution (ratio, 1:1; final concentration 0.25 mg/ml), and reanalyzed by flow cytometry after 5 min. The fluorescence of monocytes incubated with SYTO RNA-labeled TEVs was compared with control monocytes that were not incubated with TEVs. The autofluorescence of TEVs was negligible.

Flow cytometry analysis of TEVs transfer to monocyte subsets. Monocytes were stained with anti-CD14 and anti-CD16 antibodies, washed and incubated with SYTO RNA-labeled TEVs (TEV:monocyte, 5,000:1) for 15 min, 30 min or 2 h at 37˚C. Excess TEVs were washed and cells were assessed by flow cytometry by analyzing the shift in green fluorescence intensity. Due to antibody labeling, the extracellular fluorescence quenching with trypan blue was not performed. MFI and the percentage of positive cells in the FL1 channel were determined for each gated subpopulation. To determine engulfment of TEVs, monocytes stained with mAbs were separated using FACS Aria II (BD Biosciences) into three populations: i) classical ($CD14^{++}/CD16^{-}$); ii) non-classical ($CD14^{+}/CD16^{++}$) and iii) intermediate ($CD14^{++}/CD16^{+}$). Sorted cells were collected into polystyrene tubes and incubated with SYTO RNA-labeled TEVs (TEV:monocyte, 5,000:1). The experiments were performed only with HA-rich $TEVs_{HCT116}$ and limited to the shorter contact time of either 15 min or 1 h due to the small number of sorted non-classical and intermediate monocytes. The engulfment of TEVs was analyzed by quenching extracellular fluorescence with trypan blue; data are presented as a percentage of fluorescence-positive cells containing TEVs.

Blocking of CD44. The role of CD44 in TEVs endocytosis was investigated by blocking this receptor on monocytes. A total of $2x10^6$/ml monocytes were incubated with anti-CD44 mAb (cat. no. BMS113; clone no. SFF-2; 10 μg/ml; Invitrogen; Thermo Fisher Scientific, Inc) or appropriate IgG1 isotype control (cat. no. 14-4714-82; 10 μg/ml; Invitrogen; Thermo Fisher Scientific, Inc.) for 30 min at 4˚C. Monocytes were washed with RPMI, and incubated with SYTO RNA-labeled TEVs (TEV:monocyte, 5,000:1) for 30 min to 18 h at 37˚C. The binding of SYTO RNA-labeled TEVs was determined by flow cytometry. To distinguish surface-bound and internalized TEVs, the quenching of extracellular fluorescence signals by trypan blue was used. MFI value of control monocytes (without TEVs) was subtracted from the MFI of monocytes incubated with SYTO RNA-labeled TEVs (elimination of autofluorescence effect), then the MFI of monocytes incubated with SYTO RNA-labeled TEVs without blocking CD44 was established as 100% and relative to this value, the percentage change of MFI (%MFI) for monocytes with blocked CD44 or with isotype control was calculated.

In the case of monocyte subsets, binding of TEVs to monocytes for 15 min or 1 h was determined by the percentage of fluorescence-positive cells (FL1 channel) for each gated subpopulation. The engulfment of TEVs was analyzed in sorted subsets after trypan blue treatment and presented as the percentage of fluorescence-positive cells.

Statistical analysis. Statistical analysis was performed by Statistica v. 13.3 (TIBCO Software Inc.). Mann-Whitney U, Wilcoxon signed rank, Student's t-test or Welch's test were used. For multiple group comparisons, one-way ANOVA followed by Tukey's post hoc test was used. Graphs were constructed in GraphPad Prism (version 8.0.1; Dotmatics). Detailed information about the statistical tests and the number

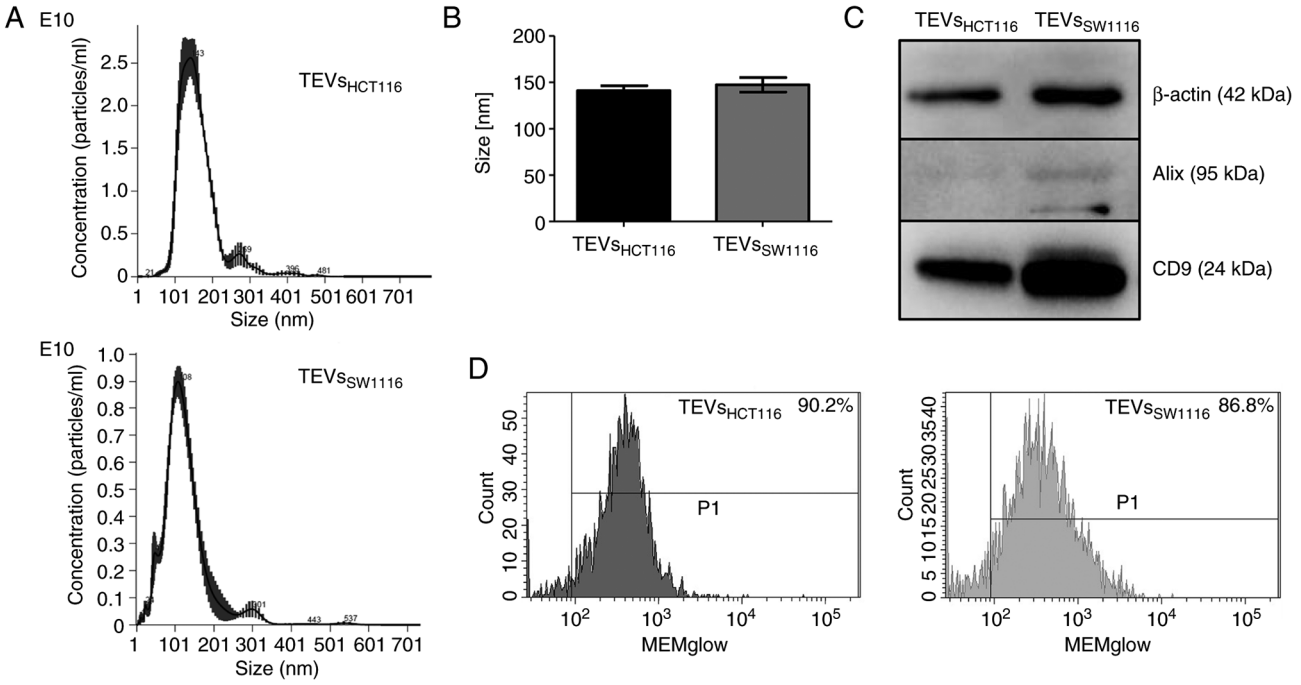

Figure 1. Characteristics of colon cancer-derived TEVs. (A) Representative NTA of the size distribution of TEVs derived from HCT116 and SW1116 cells. (B) TEVs size was determined by NTA. (C) Expression of EV markers CD9 and Alix and β-actin determined by western blotting. (D) MEMGlow staining of TEVs analyzed by flow cytometry; positive TEVs gating compared with unlabeled TEVs. TEVs, tumor-derived extracellular vesicles; NTA, nanoparticle tracking analysis.

of experiments is included in the respective figure legends. $P<0.05$ was considered to indicate a statistically significant difference.

Results

TEVs derived from colon cancer cell lines carry HA. $TEVs_{HCT116}$ and $TEVs_{SW1116}$ were isolated from cell culture supernatants by ultracentrifugation. The size distribution of TEVs was similar between $TEVs_{HCT116}$ and $TEVs_{SW1116}$ (Fig. 1A and B). Both tested TEVs expressed CD9 and β-actin as shown by WB. The expression of Alix was limited to $TEVs_{SW1116}$ (Fig. 1C). The MEMglow-positive fraction represented ~90% of both tested TEVs (Fig. 1D). The TEVs derived from HCT116 cells were significantly enriched in HA compared with those derived from SW1116 cells (200.43 vs. 0.26 ng/1x10^{11} TEVs; n=13; Fig. 2A) which was associated with HA content in cell culture supernatants (Fig. 2B; n=4). The comparison of HA levels in cultured supernatants before and after TEVs isolation indicated that HA was primarily present in soluble form. HA detected in TEVs represented only 15 and 26% of the total HA in the culture supernatants of HCT116 and SW1116 cells, respectively (Fig. 2C; n=2). There were at least two forms of CD44 (CD44s and CD44v6) present on $TEVs_{HCT116}$ (~42 and ~58%, respectively) and $TEVs_{SW1116}$ (~32 and ~44%, respectively) (data not shown).

Monocyte subsets differ in CD44 expression. To investigate the role of CD44 in interaction of monocytes with TEVs, expression of CD44 on monocytes and their subsets was determined by flow cytometry (Fig. 3A). The three monocyte subsets, classical $CD14^{++}/CD16^{-}$, intermediate $CD14^{++}/CD16^{+}$ and non-classical $CD14^{+}/CD16^{++}$, were determined based on expression of the CD14 and CD16 markers, as described by Ziegler-Heitbrock (16). Since all monocytes are $CD44^{+}$, to assess differences in CD44 expression between subsets, MFI was evaluated in comparison to the appropriate isotype control (Fig. 3B). The highest MFI of CD44 was observed in the intermediate subpopulation and only the difference between intermediate and non-classical monocytes was statistically significant (n=23). The expression of CD44 on monocytes was not affected by incubation with TEVs (data not shown) for 2 and 18 h, however, an increase in CD44 MFI was observed after 2 and 18 h of culture (Fig. S4).

Attachment and engulfment of TEVs depend on their availability, time of exposition and TEVs origin. TEVs were labeled with green fluorescent SYTO RNA Select dye. The labeling did not affect the size distribution and concentration of TEVs (Fig. S2). The efficiency of TEVs labeling was high and controlled by flow cytometry (Fig. S2). TEVs were incubated with monocytes for 30 min and 2 and 18 h, and the attachment of TEVs to monocytes was analyzed by flow cytometry. More than 90% of monocytes was fluorescence-positive after 30 min incubation with TEVs from both cell lines, thus analysis of MFI shift was considered more informative than percentage of positive cells. The increase in monocyte MFI was associated with the number of TEVs/monocyte and exposition time (Fig. S5; n=3). A TEV:monocyte ratio of 5,000:1 was chosen for further experiments. The kinetics of TEVs attachment to monocytes are shown in Fig. 4. MFI of monocytes interacting with $TEVs_{HCT116}$ increased in a shorter time compared with $TEVs_{SW1116}$. This observation may indicate higher, statistically significant efficiency of attachment of TEVs derived from

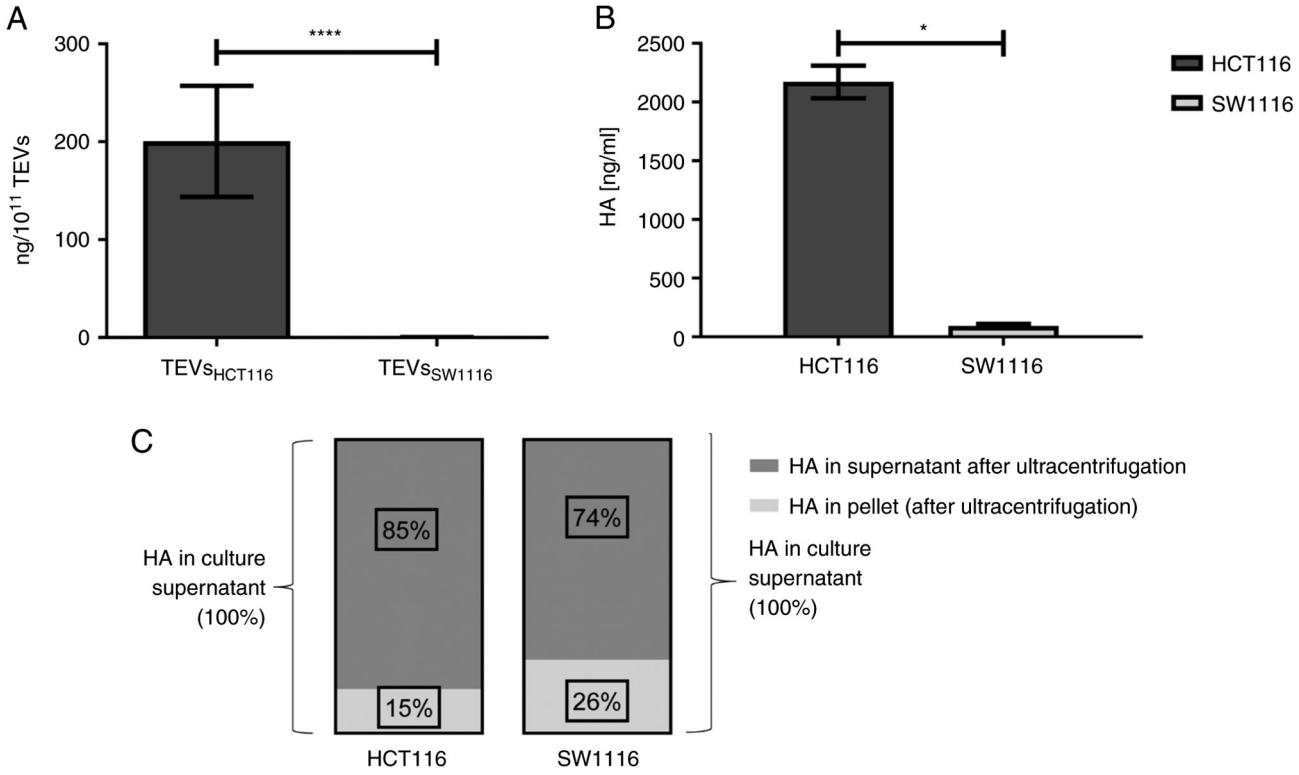

Figure 2. HA concentration in TEVs and supernatant from cell cultures. (A) $TEVs_{HCT116}$ and $TEVs_{SW1116}$ (n=13; unpaired student's t test). (B) Culture supernatants from HCT116 and SW1116 cells (n=4; Mann-Whitney U test). (C) HA content in culture supernatants and pellets following ultracentrifugation, relative to concentration of HA in culture supernatants before ultracentrifugation (n=2). Data are presented as the mean ± SEM. *P<0.05, ****P<0.0001. TEVs, tumor-derived extracellular vesicles; HA, hyaluronan.

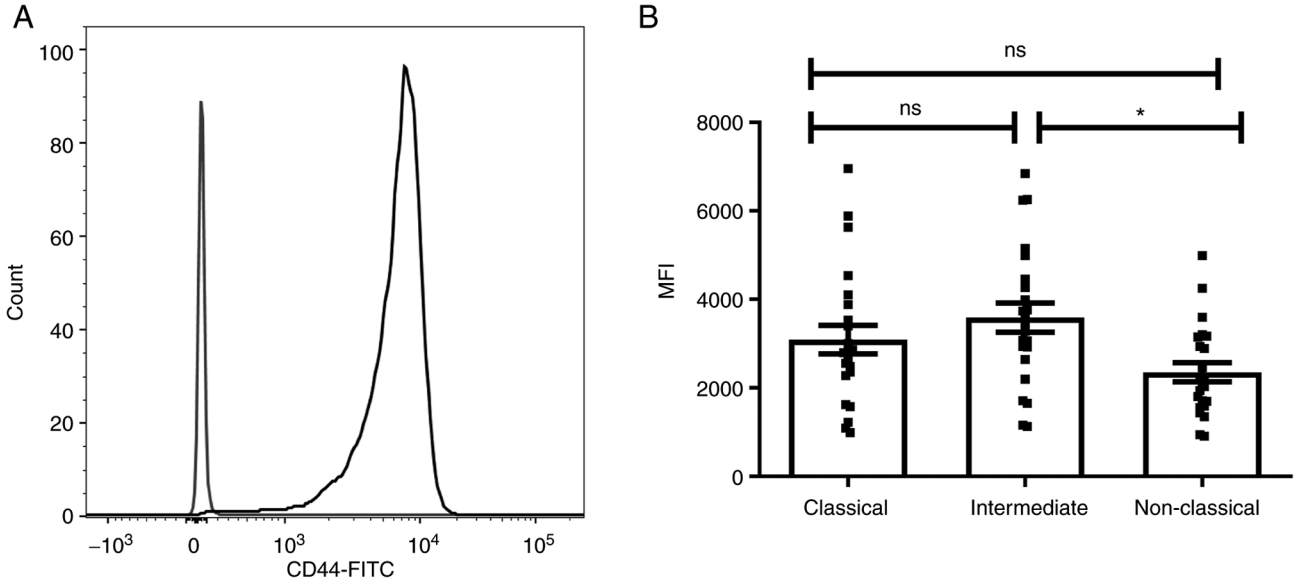

Figure 3. Expression of CD44 on monocytes and subsets. (A) Representative histogram of the whole population of human monocytes. (B) Monocyte subsets. Data are presented as the mean ± SEM (n=23). *P<0.05. Data were analyzed using ANOVA with Tukey's post hoc test. ns, non-significant; MFI, mean fluorescence intensity.

HCT116 cells compared with that of SW1116 cells (n=10; P<0.001). The percentage of monocytes showing fluorescence after 30 min incubation with $TEVs_{HCT116}$ was 5 times reduced after quenching with trypan blue (Fig. 5A). This suggested that approximately 20% of monocytes exhibited TEVs in the cytoplasmic area after that time. After 2 h incubation, ≥50% of monocytes engulfed TEVs. The internalization of $TEVs_{SW116}$ was not effective, as the uptake of TEVs after 30 min was ~3%. After 2 h, ~37% of monocytes contained $TEVs_{SW1116}$ (Fig. 5B). The internalization outcome/level of $TEVs_{HCT116}$ and $TEVs_{SW1116}$ after overnight incubation was comparable; in ~80% of monocytes, TEVs were located inside (Fig. 5; n=6).

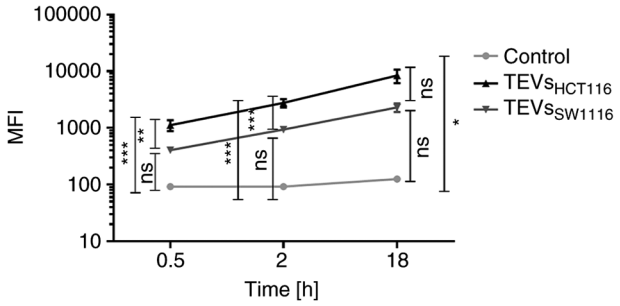

Figure 4. Kinetics of TEVs attachment/engulfment by monocytes. Monocytes were incubated with SYTO RNA-labeled TEVs. After washing, the samples were analyzed by FACSCanto. Green autofluorescence of monocytes was used as a control. Data are presented as the mean ± SEM (n=10). *P<0.05, **P<0.01 and ***P<0.001. Data were analyzed using ANOVA with Tukey's post hoc test. TEVs, tumor-derived extracellular vesicles; MFI, mean fluorescence intensity; ns, non-significant.

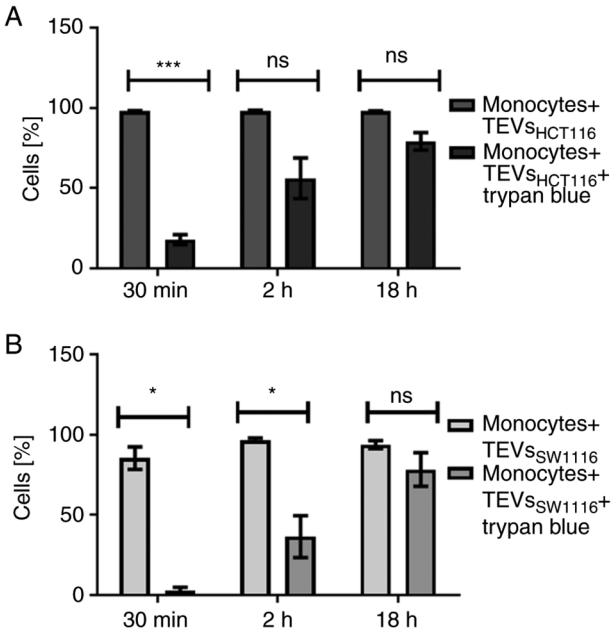

Figure 5. Internalization of TEVs by monocyte. Percentage of monocytes showing green fluorescence following incubation with SYTO RNA-labeled (A) $TEVs_{HCT116}$ and (B) $TEVs_{SW1116}$. Data are presented as the mean ± SEM (n=6). Data were analyzed using (A) paired Student's t-test or (B) Wilcoxon signed rank test. *P<0.05, ***P<0.001. TEVs, tumor-derived extracellular vesicle; ns, non-significant.

Blocking of CD44 partially inhibits HA-rich TEVs engulfment by monocytes. TEVs carry HA and are effectively engulfed by monocytes, which is associated with high expression of major HA receptor CD44. To evaluate the role of CD44 in engulfment, control monocytes and monocytes with blocked CD44 molecules were incubated with SYTO RNA-labeled TEVs. MFI of green fluorescence channel was used for quantification of TEVs attachment and engulfment following trypan blue treatment. The attachment of TEVs decreased following CD44 blocking, however this was not significant (not shown). In turn, blocking of CD44 molecules on monocytes reduced $TEVs_{HCT116}$ engulfment by 50.75% compared with that of the isotype control (P=0.00739) after 30 min incubation with TEVs; after 2 and 18 h, the reduction was 1.8 and 22.75%, respectively, but this was not significant (Fig. 6A). For $TEVs_{SW1116}$, the CD44 blocking with the short time of incubation (30 min) was skipped due to the lack of engulfment; almost all fluorescence was derived from outside of monocytes (Fig. 5B). Blocking of CD44 molecules, followed by 2 or 18 h incubation with TEVs resulted in ~27 and ~6% reduction in the % MFI, respectively, compared with the isotype control. However, the differences were not statistically significant (Fig. 6B). Isotype control did not significantly diminish TEVs engulfment compared with control monocytes (n=4).

Differences in TEVs attachment/engulfment by monocyte subsets: The role of CD44. To determine whether differences in CD44 expression on monocyte subsets affect their interactions with TEVs, MFI value of subsets was analyzed after incubation with SYTO RNA-labeled TEVs. The highest increase in MFI was observed in the intermediate subset of monocytes, which may suggest that TEVs preferentially adhere to them (Fig. 7; n=5). This observation was similar for both types of TEVs; however, MFI after incubation with $TEVs_{SW1116}$ was lower (Fig. 7), which in turn, corroborates results obtained in previous experiments (Figs. 4 and S5). Next, the percentage of monocytes in subsets that showed green fluorescence after incubation with SYTO RNA-labeled TEVs was analyzed. Following 15 min incubation with $TEVs_{HCT116}$, ~46% of classical, ~29% of intermediate and ~20% of non-classical monocytes showed green fluorescence (Fig. 8A). In the case of $TEVs_{SW1116}$, the percentages of monocytes showing green fluorescence were 7.7, 12.5 and 7.5% for classical, intermediate and non-classical monocytes, respectively (Fig. 8B). The percentages of monocytes showing green fluorescence increased over time (n=3). Blocking of CD44 on monocytes resulted in a decrease in $TEVs_{HCT116}$, but not $TEVs_{SW1116}$ binding in all three subsets by 10.1, 9.94 and 8.63% for classical, intermediate and non-classical monocytes, respectively, however, the differences were not significant and observed only after 15 min of exposure to TEVs (Fig. 8). To exclude competition between subsets of monocytes in TEVs attachment/engulfment, experiments were repeated on sorted cells. TEVs were attached and internalized by all three subsets of monocytes. After 15 min contact, the differences in TEVs attachment were slight (Fig. 9A), with a non-significant predominance of intermediate monocytes. Over time, higher binding of TEVs was observed in classical monocytes compared with that in other subsets (91 vs. 60% for classical vs. intermediate monocytes and 91 vs. 54% for classical vs. non-classical monocytes (Fig. 9B). The highest engulfment of TEVs was observed in intermediate monocytes after 15 min of incubation (Fig. 9A); the percentage of positive intermediate cells was similar before and after trypan treatment which may suggest that TEVs were effectively internalized (47 vs. 43%, respectively). Blocking of CD44 resulted in a slight reduction in binding of TEVs to classical and intermediate monocytes and stronger to non-classical monocytes (decreased by 8, 13 and 27%, respectively). The internalization of TEVs was decreased following CD44 blocking; the effect was observed for all three subsets after 15 min and 1 h of contact, however this was not significant. The percentage of fluorescence-positive classical and intermediate monocytes with blocked CD44 receptors was reduced by ~42% after quenching of extracellular fluorescence. In

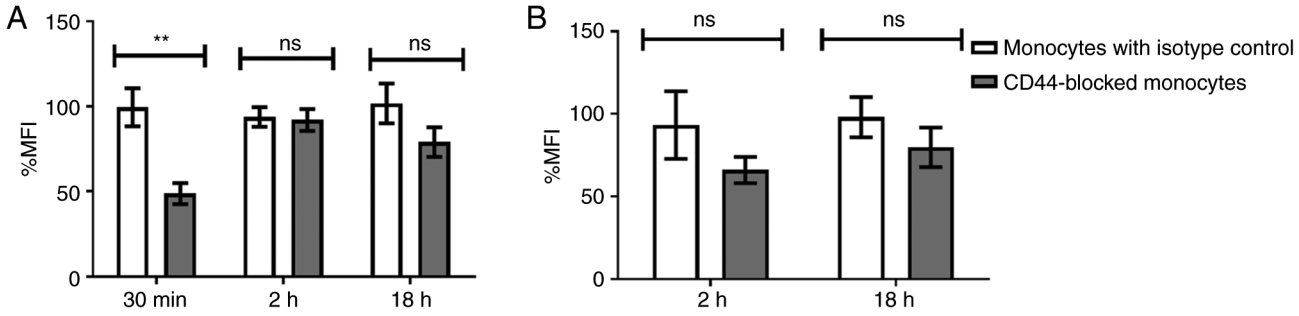

Figure 6. Percentage change in MFI of monocytes after incubation with SYTO RNA-labeled TEVs followed by extracellular fluorescence quenching with trypan blue. MFI was calculated relative to MFI of monocytes incubated with (A) $TEVs_{HCT116}$ or (B) $TEVs_{SW1116}$. Data are presented as the mean ± SEM (n=4) and analyzed using unpaired Student's or Welch's t test, respectively. **P<0.001. TEVs, tumor-derived extracellular vesicles; MFI, mean fluorescence intensity; ns, non-significant.

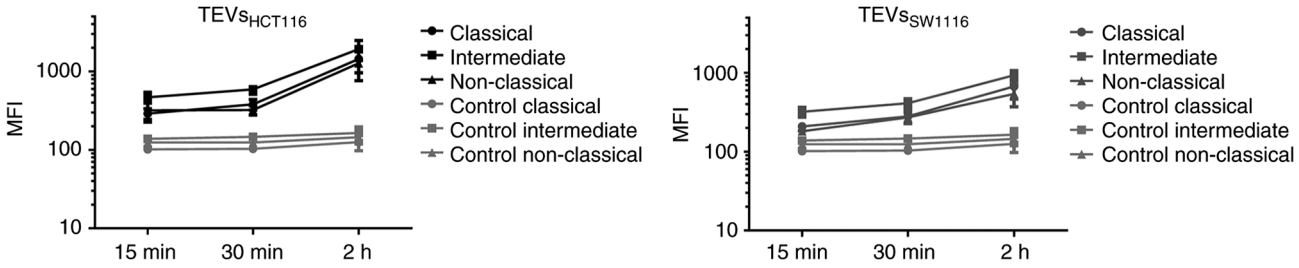

Figure 7. Kinetics of TEV attachment/engulfment by monocyte subsets. Monocytes were incubated with SYTO RNA-labeled TEVs. The samples were analyzed by FACSCanto. Green autofluorescence of monocyte subsets was used as a control. Data are presented as the mean ± SEM (n=5). The left panel represents the interaction of monocyte subsets with $TEVs_{HCT116}$ and the right panel represents $TEVs_{SW1116}$. TEVs, tumor-derived extracellular vesicles; MFI, mean fluorescence intensity.

non-classical monocytes, the decrease in the percentage of fluorescence-positive cells was ~13%.

Discussion

The present study was designed to evaluate the role of CD44 in the interactions of monocytes with colon cancer-derived EVs. TEVs released by the two colon cancer cell lines HCT116 and SW1116 were characterized. No differences in size, mode and range between $TEVs_{HCT116}$ and $TEVs_{SW1116}$ were observed; these corresponded to small EVs (24). The selective expression of EV markers suggests their mixed origin from outer and inner cell membranes (25-27). In the present study, the investigated cell lines differed in HA secretion: HCT116 cells produced more HA than SW1116 cells. Colorectal cancer cells release HA primarily in a soluble form and also in a form bound with TEVs. A major part of the sensitive cargo of TEVs is located inside and covered by membrane sheaths; however, some of the cargo may be attached to the surface. Recently, Buzas (2) and Tóth *et al* (28) described proteins and proteoglycans that 'decorate' the surface of EVs and named them 'corona'. The present study extends this observation on HA, a component of the extracellular matrix, that structurally belongs to polysaccharides. HA content in TEVs was demonstrated using ELISA and it was consistent with previous results obtained by using atomic force microscopy combined with spectroscopy (29). Paul *et al* (29) showed that $TEVs_{HCT116}$ exhibits notably increased HA surface density compared with the EVs derived from normal colon epithelium.

Elevated levels of low molecular weight HA are detected in the serum of patients with cancer, including colon cancer (30-32). According to the presented data, at least part of HA is linked with TEVs and may impact target cells via interaction with CD44. CD44 is expressed at high levels in cancer, as well as immune cells. HA supports tumor progression by promoting tumor proliferation or influencing anti-apoptotic activity (33), which is also attributed to TEVs (34). Moreover, HA promotes monocyte recruitment and redifferentiation from M1 into M2 macrophages (35), which is consistent with M2 polarization of macrophages observed after contact with TEVs (36). HA carried by TEVs may trigger changes in cell activity. Therefore, HA-rich nanoparticles may be used in targeted antitumor therapy (37), which may also impact the functions of other CD44-positive cells such as monocytes/macrophages. It was previously shown that HA-decorated liposomes improve cellular uptake and markedly inhibit proliferation of pancreatic cancer stem cells. Also, encapsulated microRNA-125b in HA-poly (ethylenimine)-based nanoparticles repolarizes TAMs from M2 to M1 in lung cancer (38).

In colon adenocarcinoma cells, HA is associated with cell surface receptors, primarily CD44 and CD44v (39). Expression of CD44 and CD44v6 on $TEVs_{HCT116}$ and $TEVs_{SW1116}$ was similar to that of EVs of other origins (data not shown) (37). TEVs from both cell lines were able to adhere to monocytes and be engulfed in a time- and dose-dependent manner. The number of TEVs/monocytes used was determined based on preliminary experiments. It was below the saturation point, however, it fit the reported average number of EVs and TEVs

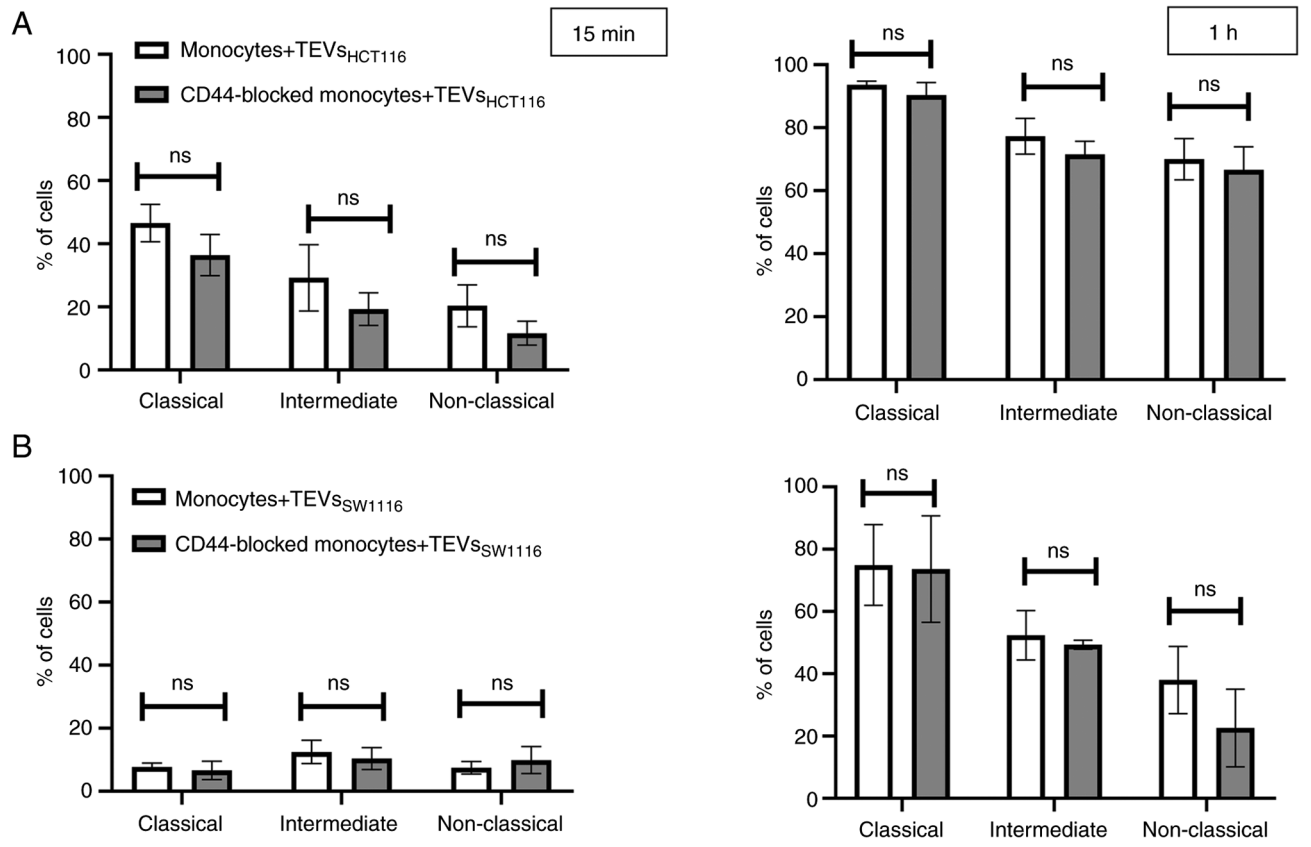

Figure 8. Attachment of TEVs to the subsets of monocytes. Percentage of monocyte subsets showing green fluorescence following incubation with SYTO RNA-labeled (A) TEVs$_{HCT116}$ or (B) TEVs$_{SW1116}$ for 15 min and 1 h. Data are presented as the mean ± SEM (n=3). Data were analyzed using Mann-Whitney U test. TEVs, tumor-derived extracellular vesicles; ns, non-significant.

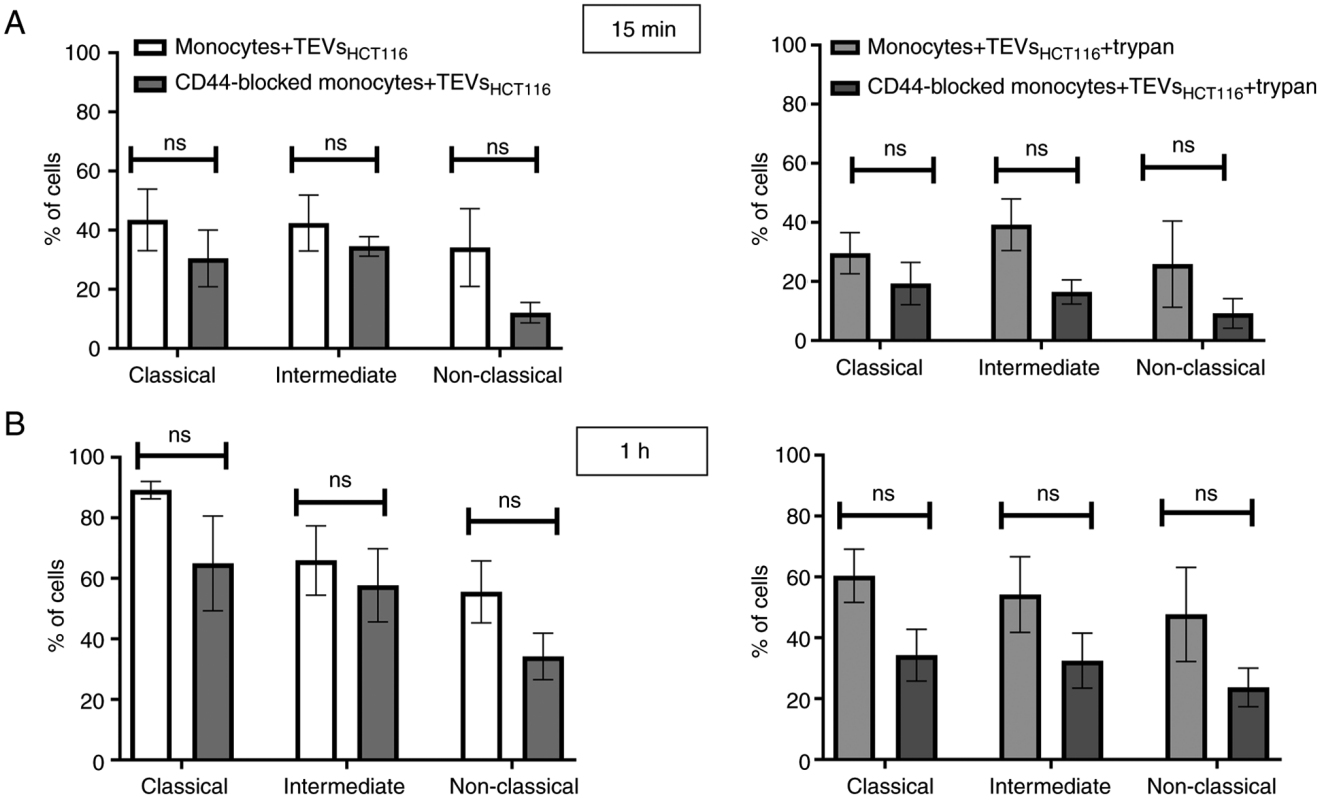

Figure 9. Internalization of TEVs by monocyte subsets. Percentage of sorted monocyte subsets showing green fluorescence after incubation with SYTO RNA-labeled TEVs$_{HCT116}$ for (A) 15 min and (B) 1 h. Data are presented as the mean ± SEM (n=3). Data were analyzed using Mann-Whitney U test. TEVs, tumor-derived extracellular vesicles.

in plasma, the average number of monocytes in the blood and the limit of detection of the flow cytometer (40,41).

Both processes of attachment and engulfment have proceeded faster and at an efficient level, as indicated by MFI value for HA-rich $TEVs_{HCT116}$, compared with HA-poor $TEVs_{SW1116}$. This observation was consistent with previous reports that the uptake of TEVs depends on their cargo. For example, expression of mucin-1 facilitates binding to dendritic cell-specific intercellular adhesion molecule-3-grabbing non-integrin (CD209) receptors on monocyte-derived dendritic cells (42) and fibronectin carried by EVs enables interaction with target cells via heparan sulfate chains (43). Previously, the spontaneous rate of EV internalization was estimated as 1% at 1 h in HeLa cells (44). The more intensive uptake of TEVs by monocytes results from high phagocytic potential and clearance capacity of pathogens and debris of cellular or other origins. TEVs are cellular derivatives, however, the mechanism of their uptake is still unclear. After 30 min incubation, ~20% of monocytes exhibited $TEVs_{HCT116}$ but not $TEVs_{SW1116}$ in the cytoplasmic area. The fast interaction corroborates the half-time of exosomes circulating in the blood (≤30 min) (45). The preferential engulfment of HA-rich TEVs directed our attention to CD44 the major HA receptor able to bind HA on immune cells (46-49). More than 90% of monocytes express the standard CD44 isoform (50). Because of the prevalence of CD44 and the absence of CD44 variant isoforms on non-activated cells, the present study was limited to this isoform. CD44 expression on monocytes was not affected by contact with TEVs (data not shown) for 2 or 18 h but increased over the culture time. Blocking of CD44 on monocytes diminished the attachment of TEVs to the cell surface and significantly decreased $TEVs_{HCT116}$ endocytosis after a short time of incubation. Previous studies suggested that HA-CD44 interaction promotes endocytosis of HA in various cell lines such as chondrocytes, keratinocytes and cancer cells (51). However, in macrophages derived from THP-1 cells, Rios de la Rosa *et al* (52) showed that the binding but not the engulfment of HA or HA-linked nanoparticles was positively associated with the expression of CD44. The differences may be due to different types of HA carriers (artificial nanoparticles vs. TEVs), the specification of cells (primary vs. differentiated from THP-1) or different dynamics of HA-CD44 complex internalization. In the present study, blocking CD44 decreased internalization of HA-rich TEVs but only in the first 30 min after contact. The lack of effect after longer contact may be due to experimental conditions such as constant concentration of blocking anti-CD44 antibody or the aforementioned increase in CD44 expression on monocytes during culture, such as caused via enhanced expression or turnover (53,54). The role of other types of endocytosis including phagocytosis, dynamin-dependent endocytosis and pinocytosis, which replace the CD44-dependent mechanism, increases over time (55-57). In $TEVs_{SW1116}$, blocking of CD44 resulted in reduced engulfment after 2 h; however, this was not statistically significant. The kinetics of the monocyte/$TEVs_{SW1116}$ interaction is similar to previously presented interactions with $TEVs_{HPC}$ derived from the pancreatic carcinoma cell line HPC-4 (20). In both $TEVs_{SW1116}$ and $TEVs_{HPC}$, the concentration of HA is notably lower compared with that in $TEVs_{HCT116}$, which results in slower internalization by monocytes (58). HA concentration as well as size of TEVs, cellular origin of HA (pancreatic vs. colon), affinity to CD44 and availability of HA (thickness of corona, presence of HA in soluble form) may impact the interactions between TEVs and target cells. The observed interaction may be important clinically as the increasing concentration of HA in the blood is considered a marker of different types of tumors, including colon cancer (30). HA-rich TEVs may be internalized in preponderance and affect polarization/functional activity of monocytes and macrophages. The present data are limited to TEVs in an *in vitro* model, whereas, in the blood, monocytes are exposed also to soluble HA, which is internalized faster than HA-coated nanoparticles (52) and may inhibit endocytosis of TEVs (59).

As monocytes are a heterogeneous population of cells, the adherence of SYTO RNA-labeled TEVs to monocyte subsets was determined. Within 1 h, almost all classical monocytes showed green fluorescence, suggesting that both types of TEVs were attached or internalized by them. Non-classical monocytes, which are poor phagocytes, interact with TEVs less effectively, especially in the case of $TEVs_{SW1116}$. TEVs were attached by an intermediate monocyte subset, whose endocytic potential was previously described (60,61). This was verified by sorted monocyte subsets and highlighted the competition between cells that may take place in the blood; classical monocytes are the most abundant subset with great phagocytic potential (60). By using sorted cells, competition between subsets of monocytes incubated with TEVs was avoided as subsets were separately incubated with TEVs. The attachment of HA-rich TEVs in subsets was comparable with a slight predominance of intermediate cells, confirming the aforementioned MFI shift after contact with SYTO RNA-labeled TEVs. Also, the highest efficiency of TEVs engulfment was observed in intermediate cells, where the smallest difference in the percentage of fluorescent cells was observed before and after trypan blue treatment after short contact with HA-rich TEVs.

Blocking of CD44 on monocytes decreased TEVs attachment in all subsets, however this was not significant. This trend was observed after a short time of contact with TEVs of 15 min, and faded over 1 h when the total population of monocytes was studied. The decrease in the attachment of TEVs to non-classical monocytes after CD44 blocking was observed only on sorted cells and may have resulted from suboptimal conditions of experiments (suboptimal concentration of blocking Ab). It is possible the concentration of anti-CD44 mAbs, which was optimized for the whole population of monocytes, was too high for non-classical cells (low CD44 expression) and suboptimal for classical and intermediate cells (high CD44 expression). Another explanation may be the different kinetics of CD44 turnover in different cells/monocytes. The endocytosis of TEVs was decreased after CD44 blocking in all subsets and associated with CD44 expression (stronger in intermediate and classical cells). It may indicate that the CD44 mechanism is more important for these subtypes of monocytes at the early stages of contact with TEVs and less notable over time, especially in classical monocytes, where it may be rapidly replaced by other types of endocytosis.

To conclude, TEVs derived from different colon cancer cell lines vary in amount of carried HA, a new 'corona' component.

The presence of HA on TEVs and other EVs might facilitate contact with target cells and trigger intracellular signaling pathways. The findings of the present study suggested that CD44 is a surface receptor important for targeting and capturing HA-rich TEVs.

Acknowledgements

Not applicable.

Funding

The present study was supported by the National Science Centre, Poland (grant no. 2019/33/B/NZ5/00647).

Availability of data and materials

The datasets used and/or analyzed during the current study are available from the corresponding author upon reasonable request.

Authors' contributions

MBK conceptualized the study. AB and MBK performed the experiments (acquisition of data), collected and analyzed data and wrote the manuscript. MS participated in the analysis and interpretation of data. AGB isolated monocytes (acquisition of data). KW performed the flow cytometry (acquisition of data). ABM, MS and KW were involved in drafting the manuscript. MBK supervised the study. MBK and MS revised the manuscript critically for important intellectual content. MBK acquired funding. MBK and AB confirm the authenticity of all the raw data. All authors have read and approved the final manuscript.

Ethics approval and consent to participate

Blood from healthy donors was purchased from the Regional Center of Blood Donation and Blood Therapy (Krakow, Poland; agreement no. DZM/SAN/CM/U-678/2015; Bioethical Committee of the Jagiellonian University, Kraków, Poland; approval no. 1072.6120.1.2020).

Patient consent for publication

Not applicable.

Competing interests

The authors declare that they have no competing interests.

References

1. Ping JYX, Neupane YR and Pastorin G: Extracellular Vesicles and Their Interplay with Biological Membranes. In: Manash KP (ed.): Extracellular Vesicles Role in Diseases, Pathogenesis and Therapy. IntechOpen Series Physiology, Volume 13, IntechOpen London, UK, pp 27-59, 2021.
2. Buzas EI: Opportunities and challenges in studying the extracellular vesicle corona. Nat Cell Biol 24: 1322-1325, 2022.
3. Chen Y, Xie Y, Xu L, Zhan S, Xiao Y, Gao Y, Wu B and Ge W: Protein content and functional characteristics of serum-purified exosomes from patients with colorectal cancer revealed by quantitative proteomics. Int J Cancer 140: 900-913, 2017.
4. Glass SE and Coffey RJ: Recent advances in the study of extracellular vesicles in colorectal cancer. Gastroenterology 163: 1188-1197, 2022.
5. Xiao Y, Zhong J, Zhong B, Huang J, Jiang L, Jiang Y, Yuan J, Sun J, Dai L, Yang C, *et al*: Exosomes as potential sources of biomarkers in colorectal cancer. Cancer Lett 476: 13-22, 2020.
6. Russell AE, Sneider A, Witwer KW, Bergese P, Bhattacharyya SN, Cocks A, Cocucci E, Erdbrügger U, Falcon-Perez JM, Freeman DW, *et al*: Biological membranes in EV biogenesis, stability, uptake, and cargo transfer: An ISEV position paper arising from the ISEV membranes and EVs workshop. J Extracell vesicles 8: 1684862, 2019.
7. Czernek L, Chworos A and Duechler M: The uptake of extracellular vesicles is affected by the differentiation status of myeloid cells. Scand J Immunol 82: 506-514, 2015.
8. Popēna I, Ābols A, Saulīte L, Pleiko K, Zandberga E, Jēkabsons K, Endzeliņš E, Llorente A, Linē A and Riekstiņa U: Effect of colorectal cancer-derived extracellular vesicles on the immunophenotype and cytokine secretion profile of monocytes and macrophages. Cell Commun Signal 16: 17, 2018.
9. Baj-Krzyworzeka M, Szatanek R, Weglarczyk K, Baran J, Urbanowicz B, Brański P, Ratajczak MZ and Zembala M: Tumour-derived microvesicles carry several surface determinants and mRNA of tumour cells and transfer some of these determinants to monocytes. Cancer Immunol Immunother 55: 808-818, 2006.
10. Kwok ZH, Wang C and Jin Y: Extracellular vesicle transportation and uptake by recipient cells: A critical process to regulate human diseases. Processes (Basel) 9: 273, 2021.
11. Dale DC, Boxer L and Conrad Liles W: The phagocytes: Neutrophils and monocytes. Blood 112: 935-945, 2008.
12. Uribe-Querol E and Rosales C: Phagocytosis: Our current understanding of a universal biological process. Front Immunol 11: 1066, 2020.
13. Vachon E, Martin R, Plumb J, Kwok V, Vandivier RW, Glogauer M, Kapus A, Wang X, Chow CW and Grinstein S: CD44 is a phagocytic receptor. Blood 107: 4149-4158, 2006.
14. Szatanek R and Baj-Krzyworzeka M: CD44 and tumor-derived extracellular vesicles (TEVs). Possible gateway to cancer metastasis. Int J Mol Sci 22: 1463, 2021.
15. Ziegler-Heitbrock L, Ancuta P, Crowe S, Dalod M, Grau V, Hart DN, Leenen PJ, Liu YJ, MacPherson G, Randolph GJ, *et al*: Nomenclature of monocytes and dendritic cells in blood. Blood 116: e74-e80, 2010.
16. Ziegler-Heitbrock L: Blood monocytes and their subsets: Established features and open questions. Front Immunol 6: 423, 2015.
17. Fu X and Yin M: Monocytes in tumor: The perspectives of single-cell analysis. Tumor Discov 1: 4, 2022.
18. Turrini R, Pabois A, Xenarios I, Coukos G, Delaloye JF and Doucey MA: Tie-2 expressing monocytes in human cancers. Oncoimmunology 6: e1303585, 2017.
19. Cormican S and Griffin MD: Human monocyte subset distinctions and function: Insights from gene expression analysis. Front Immunol 11: 1070, 2020.
20. Baj-Krzyworzeka M, Weglarczyk K, Szatanek R, Mytar B, Baran J and Siedlar M: The role of CD44H molecule in the interactions between human monocytes and pancreatic adenocarcinoma-derived microvesicles. Folia Histochem Cytobiol 57: 28-34, 2019.
21. Zembala M, Siedlar M, Ruggiero I, Wieckiewicz J, Mytar B, Mattei M and Colizzi V: The MHC class-II and CD44 molecules are involved in the induction of tumour necrosis factor (TNF) gene expression by human monocytes stimulated with tumor cells. Int J Cancer 56: 269-274, 1994.
22. Hyenne V, Ghoroghi S, Collot M, Bons J, Follain G, Harlepp S, Mary B, Bauer J, Mercier L, Busnelli I, *et al*: Studying the fate of tumor extracellular vesicles at high spatiotemporal resolution using the zebrafish embryo. Dev Cell 48: 554-572.e7, 2019.
23. Chaka W, Scharringa J, Verheul AFM, Verhoef J, Van Strijp AG and Hoepelman IM: Quantitative analysis of phagocytosis and killing of Cryptococcus neoformans by human peripheral blood mononuclear cells by flow cytometry. Clin Diagn Lab Immunol 2: 753-759, 1995.
24. Théry C, Witwer KW, Aikawa E, Alcaraz MJ, Anderson JD, Andriantsitohaina R, Antoniou A, Arab T, Archer F, Atkin-Smith GK, *et al*: Minimal information for studies of extracellular vesicles (MISEV2018): A position statement of the international society for extracellular vesicles and update of the MISEV2014 guidelines. J Extracell vesicles 7: 1535750, 2018.

25. Kowal J, Arras G, Colombo M, Jouve M, Morath JP, Primdal-Bengtson B, Dingli F, Loew D, Tkach M and Théry C: Proteomic comparison defines novel markers to characterize heterogeneous populations of extracellular vesicle subtypes. Proc Natl Acad Sci USA 113: E968-E977, 2016.
26. Khan SA, Tyagi M, Sharma AK, Barreto SG, Sirohi B, Ramadwar M, Shrikhande SV and Gupta S: Cell-type specificity of β-actin expression and its clinicopathological correlation in gastric adenocarcinoma. World J Gastroenterol 20: 12202-12211, 2014.
27. Pols MS and Klumperman J: Trafficking and function of the tetraspanin CD63. Exp Cell Res 315: 1584-1592, 2009.
28. Tóth EÁ, Turiák L, Visnovitz T, Cserép C, Mázló A, Sódar BW, Försönits AI, Petővári G, Sebestyén A, Komlósi Z, *et al*: Formation of a protein corona on the surface of extracellular vesicles in blood plasma. J Extracell vesicles 10: e12140, 2021.
29. Paul D, Roy A, Nandy A, Datta B, Borar P, Pal SK, Senapati D and Rakshit T: Identification of biomarker hyaluronan on colon cancer extracellular vesicles using correlative AFM and spectroscopy. J Phys Chem Lett 11: 5569-5576, 2020.
30. Zhang G, Lu R, Wu M, Liu Y, He Y, Xu J, Yang C, Du Y and Gao F: Colorectal cancer-associated ~ 6 kDa hyaluronan serves as a novel biomarker for cancer progression and metastasis. FEBS J 286: 3148-3163, 2019.
31. Ropponen K, Tammi M, Parkkinen J, Eskelinen M, Tammi R, Lipponen P, Agren U, Alhava E and Kosma VM: Tumor cell-associated hyaluronan as an unfavorable prognostic factor in colorectal cancer. Cancer Res 58: 342-347, 1998.
32. Josefsson A, Adamo H, Hammarsten P, Granfors T, Stattin P, Egevad L, Laurent AE, Wikström P and Bergh A: Prostate cancer increases hyaluronan in surrounding nonmalignant stroma, and this response is associated with tumor growth and an unfavorable outcome. Am J Pathol 179: 1961-1968, 2011.
33. Karousou E, Misra S, Ghatak S, Dobra K, Götte M, Vigetti D, Passi A, Karamanos NK and Skandalis SS: Roles and targeting of the HAS/hyaluronan/CD44 molecular system in cancer. Matrix Biol 59: 3-22, 2017.
34. Baj-Krzyworzeka M, Mytar B, Weglarczyk K, Szatanek R, Kijowski J and Siedlar M: Protumorogenic potential of pancreatic adenocarcinoma-derived extracellular vesicles. Folia Biol (Praha) 66: 104-110, 2020.
35. Liu M, Tolg C and Turley E: Dissecting the dual nature of hyaluronan in the tumor microenvironment. Front Immunol 10: 947, 2019.
36. Baj-Krzyworzeka M, Mytar B, Szatanek R, Surmiak M, Węglarczyk K, Baran J and Siedlar M: Colorectal cancer-derived microvesicles modulate differentiation of human monocytes to macrophages. J Transl Med 14: 36, 2016.
37. Rilla K, Siiskonen H, Tammi M and Tammi R: Hyaluronan-coated extracellular vesicles-a novel link between hyaluronan and cancer. Adv Cancer Res 123: 121-148, 2014.
38. Luo Z, Dai Y and Gao H: Development and application of hyaluronic acid in tumor targeting drug delivery. Acta Pharm Sin B 9: 1099-1112, 2019.
39. Heider KH, Hofmann M, Hors E, van den Berg F, Ponta H, Herrlich P and Pals ST: A human homologue of the rat metastasis-associated variant of CD44 is expressed in colorectal carcinomas and adenomatous polyps. J Cell Biol 120: 227-233, 1993.
40. He M and Zeng Y: Microfluidic exosome analysis toward liquid biopsy for cancer. J Lab Autom 21: 599-608, 2016.
41. Johnsen KB, Gudbergsson JM, Andresen TL and Simonsen JB: What is the blood concentration of extracellular vesicles? Implications for the use of extracellular vesicles as blood-borne biomarkers of cancer. Biochim Biophys Acta Rev Cancer 1871: 109-116, 2019.
42. Näslund TI, Paquin-Proulx D, Paredes PT, Vallhov H, Sandberg JK and Gabrielsson S: Exosomes from breast milk inhibit HIV-1 infection of dendritic cells and subsequent viral transfer to CD4+ T cells. AIDS 28: 171-180, 2014.
43. Purushothaman A, Bandari SK, Liu J, Mobley JA, Brown EE and Sanderson RD: Fibronectin on the surface of myeloma cell-derived exosomes mediates exosome-cell interactions. J Biol Chem 291: 1652-1663, 2016.
44. Bonsergent E, Grisard E, Buchrieser J, Schwartz O, Théry C and Lavieu G: Quantitative characterization of extracellular vesicle uptake and content delivery within mammalian cells. Nat Commun 12: 1864, 2021.
45. Yamashita T, Takahashi Y, Nishikawa M and Takakura Y: Effect of exosome isolation methods on physicochemical properties of exosomes and clearance of exosomes from the blood circulation. Eur J Pharm Biopharm 98: 1-8, 2016.
46. Gouëffic Y, Guilluy C, Guérin P, Patra P, Pacaud P and Loirand G: Hyaluronan induces vascular smooth muscle cell migration through RHAMM-mediated PI3K-dependent Rac activation. Cardiovasc Res 72: 339-348, 2006.
47. Schledzewski K, Falkowski M, Moldenhauer G, Metharom P, Kzhyshkowska J, Ganss R, Demory A, Falkowska-Hansen B, Kurzen H, Ugurel S, *et al*: Lymphatic endothelium-specific hyaluronan receptor LYVE-1 is expressed by stabilin-1+, F4/80+, CD11b+ macrophages in malignant tumours and wound healing tissue in vivo and in bone marrow cultures in vitro: Implications for the assessment of lymphangiogene. J Pathol 209: 67-77, 2006.
48. Taylor KR, Yamasaki K, Radek KA, Nardo AD, Goodarzi H, Golenbock D, Beutler B and Gallo RL: Recognition of hyaluronan released in sterile injury involves a unique receptor complex dependent on Toll-like receptor 4, CD44, and MD-2. J Biol Chem 282: 18265-18275, 2007.
49. Lee-Sayer SSM, Dong Y, Arif AA, Olsson M, Brown KL and Johnson P: The where, when, how, and why of hyaluronan binding by immune cells. Front Immunol 6: 150, 2015.
50. Khaldoyanidi S, Achtnich M, Hehlmann R and Zöller M: Expression of CD44 variant isoforms in peripheral blood leukocytes in malignant lymphoma and leukemia: Inverse correlation between expression and tumor progression. Leuk Res 20: 839-851, 1996.
51. Choi KY, Saravanakumar G, Park JH and Park K: Hyaluronic acid-based nanocarriers for intracellular targeting: Interfacial interactions with proteins in cancer. Colloids Surf B Biointerfaces 99: 82-94, 2012.
52. Rios de la Rosa JM, Tirella A, Gennari A, Stratford IJ and Tirelli N: The CD44-mediated uptake of hyaluronic acid-based carriers in macrophages. Adv Healthc Mater 6: 1601012, 2017.
53. Goebeler M, Kaufmann D, Bröcker EB and Klein CE: Migration of highly aggressive melanoma cells on hyaluronic acid is associated with functional changes, increased turnover and shedding of CD44 receptors. J Cell Sci 109: 1957-1964, 1996.
54. Shi M, Dennis K, Peschon JJ, Chandrasekaran R and Mikecz K: Antibody-induced shedding of CD44 from adherent cells is linked to the assembly of the cytoskeleton. J Immunol 167: 123-131, 2001.
55. Parada N, Romero-Trujillo A, Georges N and Alcayaga-Miranda F: Camouflage strategies for therapeutic exosomes evasion from phagocytosis. J Adv Res 31: 61-74, 2021.
56. Mulcahy LA, Pink RC and Carter DR: Routes and mechanisms of extracellular vesicle uptake. J Extracell vesicles 3: 10.3402/jev.v3.24641, 2014.
57. Bjørnetrø T, Steffensen LA, Vestad B, Brusletto BS, Olstad OK, Trøseid AM, Aass HCD, Haug KBF, Llorente A, Bøe SO, *et al*: Uptake of circulating extracellular vesicles from rectal cancer patients and differential responses by human monocyte cultures. FEBS Open Bio 11: 724-740, 2021.
58. Lenart M, Rutkowska-Zapala M, Baj-Krzyworzeka M, Szatanek R, Węglarczyk K, Smallie T, Ziegler-Heitbrock L, Zembala M and Siedlar M: Hyaluronan carried by tumor-derived microvesicles induces IL-10 production in classical (CD14++CD16-) monocytes via PI3K/Akt/mTOR-dependent signaling pathway. Immunobiology 222:1-10, 2017.
59. Jordan AR, Racine RR, Hennig MJ and Lokeshwar VB: The role of CD44 in disease pathophysiology and targeted treatment. Front Immunol 6: 182, 2015.
60. Kapellos TS, Bonaguro L, Gemünd I, Reusch N, Saglam A, Hinkley ER and Schultze JL: Human monocyte subsets and phenotypes in major chronic inflammatory diseases. Front Immunol 10: 2035, 2019.
61. Kwong C, Gilman-Sachs A and Beaman K: An independent endocytic pathway stimulates different monocyte subsets by the a2 N-terminus domain of vacuolar-ATPase. Oncoimmunology 2: e22978, 2013.